OPTIMIZATION OF A HIGH POWER 2.3 Mm YB:TM:YLF LASER, SIMULTANEOUSLY DIODE-PUMPED AT 685 nm AND 960 nm

N. U. Wetter, P. S. F. de Matos, S. L. Baldochi, I. M. Ranieri
Centro de Lasers e Aplicações, IPEN/SP
Av. Prof. Lineu Prestes, 2242, São Paulo 05508-900 Brazil, tel: +55 11 3816 9305, e-mail: nuwetter@ipen.br

RESUMO

É demonstrado um laser de Yb:Tm:YLF emitindo em 2.3 µm bombeado simultâneamente em 685 nm e 960 nm, resultando em maior eficiência que o bombeamento único em 960 nm. Mostramos a melhor relação entre as potências de bombeamento em 685 nm e 960 nm. A potência de saída de 620 mW é a maior já reportada.

ABSTRACT

Simultaneous pumping of the 2.3 µm Yb:Tm:YLF laser at 685 nm and 960 nm is demonstrated, showing higher slope efficiency than 960 nm alone. The best relation between 685 nm pump power and 960 nm pump power is shown. The output power of 620 mW is the highest reported so far.

Descritores: *lasers, bombeamento por diodo, YbTm:YLF*

Key words: *laser, diode-pumped, Yb:Tm:YLF*

INTRODUCTION

Tunable lasers emitting around 2.3 µm region are important in many application areas. They are especially of interest in gas detection [1,2] systems, because of the presence of strong absorption lines of atmospheric pollutants in the spectral region around 2.3 µm such as CO, CH_4 and HF. The 2.3 µm laser is used for sensing carbon monoxide and hydrocarbon gases in combustion experiments and LIDAR applications [3], in part because of its relatively weak water vapor absorption. In situ absorption measurements of CO concentration in combustion experiments have shown a minimum detectivity of less than 10 ppm using 2.3 µm radiation. Lasers in the region 2.0-2.5 µm play also an important role in noninvasive blood glucose measurements [4].

Thulium has a large emission spectra around 2.3 µm with demonstrated tuning range of 2.2-2.45 µm using the YLF host [5]. Tm:YLF has strong absorption lines at 685 and 780 nm that are accessible with diode lasers. The absorption at 685 nm is three times larger than that at 780 nm [6]. With the commercial availability of high power (up to 5 W) diode lasers emitting at 685 nm, this pumping wavelength is of interest because it permits much more effective pump arrangements due to the higher absorption coefficient.

Due to a highly concentration dependent cross-relaxation process that leads to a reduction of the 2.3 micron emission from the upper laser level, the thulium concentration should be kept below 2 mol % [5]. For efficient pump absorption, a high concentration sensitizer like ytterbium can be used. Yb can be diode-pumped at 960 nm where high-power diodes are available. We have already demonstrated quasi-cw operation of the Yb:Tm:YLF laser, pumped at 960 nm with a 20 W diode bar achieving the highest output power reported so far of 520 mW [7].

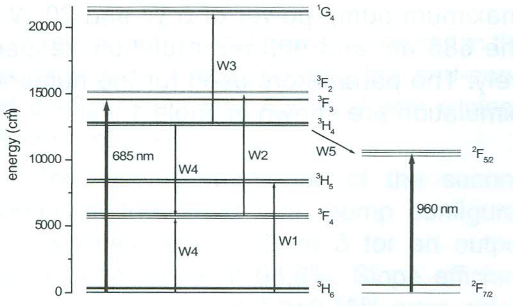

Figure1: Energy-level scheme of Yb:Tm:YLF. W1, W2, W3 represent energy transfer upconversions; W4 is a cross-relaxation and W5 a back-transfer.

In the 960 nm Yb:Tm pumping scheme occur three (W1,W2,W3) energy transfer upconversion processes (ETU) as illustrated in Figure 1. After pump excitation from the $^2F_{7/2}$ level to the $^2F_{5/2}$ level, the ytterbium transfers its energy to the $^3H_5$ Tm level, followed by a fast multi-phonon relaxation down to the metastable $^3F_4$ level. A second ETU process to the $^3F_2$ energy level of Tm^{3+} followed by a rapid relaxation populates the upper laser level ($^3H_4$). The next ETU causes losses to the system because it transfers population from the upper laser level into the $^1G_4$ level of Tm. Other processes deplete the upper laser level: the non-radiative transfer via cross-relaxation originating from the $^3H_4$ and $^3H_6$ levels to the $^3F_4$ level (W4) and the back-transfer (W5) from the $^3H_4$ thulium level to $^2F_{5/2}$ ytterbium level.

Laser action at 2.3 micron in Tm is based on the $^3H_4$-$^3H_5$ transition. In the 685 nm pumping scheme, Tm is pumped from the $^3H_6$ ground state into $^3F_3$ manifold followed by a fast multi-phonon relaxation to the upper laser lavel $^3H_4$. There exists also excited state absorption from $^3F_3$ into $^1D_2$ followed by a blue emission at 450 nm.

This works studies the Yb:Tm system pumped at 685 nm and 960 nm simultaneously.

EXPERIMENTAL SETUP

The Yb:Tm:YLF crystals were grown at our in-home crystal growth facility with a concentration of 9.5 mol % ytterbium and 1.2 mol% thulium. These concentrations allow for maximum efficiency of the 2.3 μm emission [8]. Growth was done by the Czochralski method in a closed system using resistive heating and a reactive atmosphere. The Brewster crystal was mounted on a water-cooled copper heat-sink. Its length was 4.6 mm and it absorbed 96% of the 960 nm pump radiation. The laser cavity length was 2.3 cm using a 10 cm radius-of-curvature high-reflectivity input mirror and a flat output coupler.

The crystal was first end-pumped by a 20 W diode bar at 960 nm and later both, end-pumped and side-pumped, by a 5 W diode bar at 685 nm as show in Figure 2. For the end-pumping setup, a series of lenses and a two-mirror beamshaper were used to reconfigure the diode emission into a more circular beam with approximately equal M^2 factors in the x- and y-direction [9]. A pump intensity of 19 kW/cm^2 and a M^2 quality factor of 42x29 (horizontal x vertical) were achieved at the crystal position as measured with a calibrated power meter and a CCD, using the second moment method to calculate the beam spot sizes. Pump spot size was 310 x 230 μm^2. Due to losses in the beamshaper and the input mirror, the maximum pump power was 11 W.

For the 685 nm, side-pumped set-up, we used a half-wave-plate to rotate the diode's emission parallel to the crystal's c-axis in order to access its high absorption coefficient of 4.3 cm^{-1} (1 mol% doping). The pump beam was incident on the top surface of the crystal. A 3 cm spherical lens and mirror at 45 degrees matched the pump beam to the laser mode size inside the crystal. Due to losses, the maximum pump power was 4.5 W. An indium foil between the crystal and the heat-sink reflected the 685 nm pump beam back into to the laser mode. We estimated a total absorbed pump power of 600 mW in this double-pass, side-pumped configuration. In order to allow the 685 nm pump beam to access the crystal from the top we could not remove the generated heat from the crystal's top face and had to use qcw operation. Pulse durations ranged from 2 ms to 10 ms at 10 to 40 Hz.

In order to establish which fraction of 685 nm pump power achieves the highest output power, we used a numerical, time resolved simulation which included all energy-levels of Figure 1. The system of eight differential, non-linear equations is solved using a second order Fehlberg algorithm. Also, it is assumed that the crystal is longitudinally pumped from both sides with the same pump parameters as described above, except for a maximum pump power of 5 W and 20 W for the 685 nm and 960 nm radiation, respectively. The parameters used for the numerical simulation are shown in Table 1.

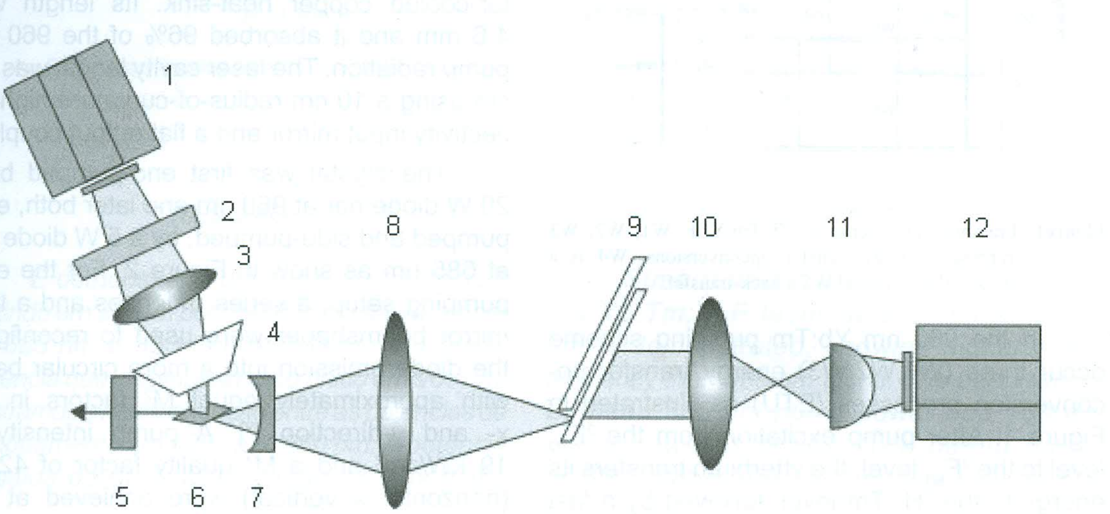

Figure 2. Pumping scheme: (1) 685 nm diode laser; (2) λ/2 waveplate; (3) spherical lens; (4) folding mirror; (5) output coupler; (6) Brewster cut Yb:Tm:YLF crystal; (7) input mirror; (8) spherical lens; (9) two-mirror beam-shaper; (10) spherical lens; (11) cylindrical lens; (12) 960 nm diode laser.

Table 1: Parameters used in the numerical simulation.

fluorescence lifetime $^3F_{5/2}$	$0.57\text{x}10^{-3}$
fluorescence lifetime $^3F_4$	$15\text{x}10^{-3}$
fluorescence lifetime $^3H_5$	$1\text{x}10^{-6}$
fluorescence lifetime $^3H_4$	$0.6\text{x}10^{-3}$
fluorescence lifetime $^1G_4$	$0.54\text{x}10^{-3}$
branching ratio $^3H_4 \rightarrow {}^3H_6$	0.924
branching ratio $^1G_4 \rightarrow {}^3H_6$	0.406
branching ratio $^3H_4 \rightarrow {}^3F_4$	0.07
branching ratio $^1G_4 \rightarrow {}^3F_4$	0.076
branching ratio $^3H_4 \rightarrow {}^3H_5$	0.006
branching ratio $^1G_4 \rightarrow {}^3H_5$	0.366
branching ratio $^1G_4 \rightarrow {}^3H_4$	0.155
active center number density for 9 mol% Yb	$12.4\text{x}10^{20}$ cm^{-3}
active center number density for 1.3 mol% Tm	$1.5\text{x}10^{20}$ cm^{-3}
energy transfer upconversion W1	$1.054\text{x}10^{-17}$ cm^3/s
energy transfer upconversion W2	$2.728\text{x}10^{-17}$ cm^3/s
energy transfer upconversion W3	$2.480\text{x}10^{-17}$ cm^3/s
cross-relaxation rate W4	$3.450\text{x}10^{-18}$ cm^3/s
back-transfer rate W5	$8.700\text{x}10^{19}$ cm^3/s
laser emission cross section	$1.2\text{x}10^{-20}$ cm^2
effective pump absorption cross section at 960 nm and 25 ºC	$7.0\text{x}10^{-21}$ cm^2
effective pump absorption cross section at 685 nm and 25 ºC	$2.2\text{x}10^{-20}$ cm^2
upper pump level Bolzmann occupation factor	0.30
lower pump level Bolzmann occupation factor	0.62
upper laser level Bolzmann occupation factor	0.19
lower laser level Bolzmann occupation factor (second highest Stark level of $^3H_5$)	0.28
degeneracy of upper laser level	1
degeneracy of lower laser level	2
pump delivery efficiency	0.625
mode fill efficiency	0.77
double pass cavity transmission	0.98
output mirror reflectivity	0.988
fraction of spontaneous emission coupled into laser mode	$1.6\text{x}10^{-5}$
radiatively emitted decay rate from upper laser level to lower laser level	0.006 s^{-1}

RESULTS AND DISCUSSION

The highest output power, achieved in the first experiment that used only the end-pumped configuration, was 620 mW with a slope efficiency of 8%.

The laser performance of the second experiment that used both pump configurations is illustrated in Figure 3 for an output coupler reflectance of 98,8%. Slope efficiencies of 7,3±0.15% and 7,9±0.15% were obtained for single and double pumping, respectively. For the double pumping scheme, the 685 nm diode is fixed at 5 W output power and only the 960 nm pump is varied. The x-axis shows the total absorbed pump power. The threshold pump power reduced from 3.0 W to 2.6 W for dual pumping, although care must be taking with this information, because a large error margin is involved in the estimate of the absorbed 685 nm pump power.

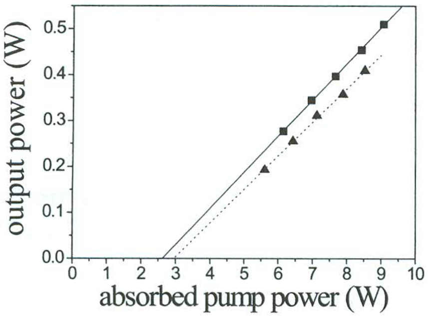

Figure 3: Output power of the Yb:Tm:YLF at 2.3 μm as a function of input power.

Another interesting characteristic of the double pumping scheme is that the laser turn-on time reduces from 1.0 ms in the single pumping scheme to 0.82 ms in the double pumping scheme. Because resonator losses are the same in both cases, this demonstrates a higher small signal gain when using 685 nm.

The numerical simulations showed a clear maximum for the optimum fraction of 685 nm pump power of about 35% (Figure 4). The significant increase in output power of almost 33% is obtained. It should be remarked that the optimum fraction of 685 nm pump power is a function of pump absorption efficiency and therefore depends on pump parameters as well as crystal doping and geometry. The simulation also demonstrates clearly that pure 685 nm pumping is inefficient due to the bottleneck effect of the $^3F_4$ energy level.

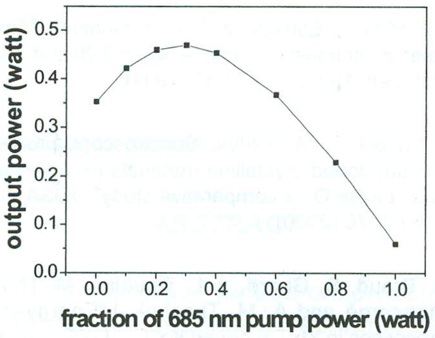

Figure 4: Numerical simulation of the output power as a function of the fraction of 685 nm pump power maintaining a total input power of 25 watt.

CONCLUSIONS

Yb:Tm:YLF laser operation at 2.3 μm, achieved by pumping simultaneously at 685 nm and 960 nm, is demonstrated. The output power of 620 mW is, to our knowledge, the highest reported so far. Higher slope efficiency is achieved for double pumping with 685 nm and an increase in output power of more than 30% seems possible if a total pump power fraction of 35% 685 nm pump radiation is used.

ACKNOWLEDGMENTS

We are thankful to the CNPq and FAPESP for the financial support of this work.

REFERENCES

[1] F. J. McAleavey, J. O'Gorman, J. F. Donegan, J. Hegarty and G. Maze, "Extremely high sensitivity gas detection at 2.3 μm using a grazing incidence Tm^{3+} fibre laser cavity", Sensors and Actuators A 87, 107-112 (2001)

[2] L. Cerutti, A. Garnache, A. Ouvrard, M. Garcia and F. Genty, "Vertical cavity surface emitting laser sources for gas detection", Phys. Stat. Sol. A 2002 (4), 631-635 (2005)

[3] Webber ME, Wang J, Sanders ST, Baer DS, Hanson RK. In situ combustion measurements of CO, CO2, H2O and temperature using diode laser absorption sensors. Proceedings Of The Combustion Institute 28: 407-413 Part 1 (2000).

[4] J. T. Olesberg C. Mermelstein, J. Schmitz and J. Wagner, “Tunable laser diode system for noninvasive blood glucose measurements” in Optical Diagnostics and Sensing V , A. V. Priezzhev and G. L. Cote, eds, Proc. SPIE 5702, 23-29 (2005)

[5] J. F. Pinto, L. Esterowitz, G. H. Rosenblatt, “Tm^{3+}:YLF laser continuously tunable between 2.20 and 2.46 µm”, Opt. Lett. 19 (12), 683-685 (1994)

[6] V. Sudesh, E. M. Goldys, “Spectroscopic properties of thulium-doped crystalline materials including a novel host, $La_2Be_2O_5$: a comparative study”, JOSA B 17 (6), 1068-1076 (2000)

[8]A. Braud, S. Girard, J. L. Doualan, M. Thuau, R. Moncorgé and A. M. Tkachuk, “Energy-transfer processes in Yb:Tm-doped KY_3F_{10}, $LiYF_4$, and BaY_2F_8 single crystals for laser operation at 1.5 and 2.3 µm”, Phys. Rev. B 61 (8), 5280-5292 (2000)

[9] W. A. Clarkson and D. C. Hanna, “Efficient Nd:YAG laser end pumped by a 20-W diode-laser bar”, Opt. Lett. 21 (12), 869-871 (1996)